

## LAB 2

### BEAM BENDING TO MEASURE ELASTIC MODULUS

#### Katherine Hom

Undergraduate Student  
Mechanical Engineering  
University of California  
Berkeley, California 94704

#### Cozmo Nakamura

Undergraduate Student  
Mechanical Engineering  
University of California  
Berkeley, California 94704

#### Adolfo Tec

Undergraduate Student  
Mechanical Engineering  
University of California  
Berkeley, California 94704

#### ABSTRACT

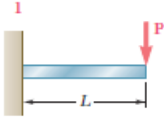
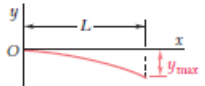
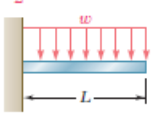
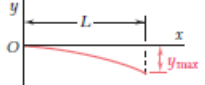
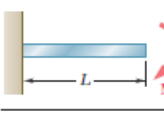
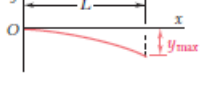
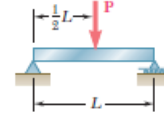
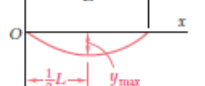
*This lab involves the use of a three point flexural test to measure the deflection that occurs under a specific load, in order to calculate the Young's (elastic) modulus. The goal of the lab is to assess the validity and accuracy of this methodology with the available lab equipment, and determine the effects of the propagation of uncertainty for our results. The results illustrated that the tests were not accurate enough to achieve the desired Young's modulus value, with only one of the samples coming close to do so. In further iterations of this lab, finer measuring tools and additional samples should be used to reach the desired Young's modulus values.*

#### INTRODUCTION

Young's modulus ( $E$ ) is a measure of stiffness, representing how well a material bends or stretches. Knowledge of a material's elastic modulus is useful in engineering for choosing the appropriate material based on its application. Each material has a set Young's modulus which can be referenced in books or online sources. However, many references do not include how accurate or uncertain their documented value is. This poses a problem because often times in engineering a material's property must be known to a certain accuracy to avoid failures.

To obtain the Young's modulus of a material, beam bending has been proposed to be an effective experiment. In order to validate this, a few aluminum samples of varying thicknesses were taken for testing under a three point bend test. A shop vise mounted with a compression load cell and linear optical encoder were used to collect data during beam bending. Once calibrated,

the displacement and load force data from the sensors can be collected on a LabView VI. With precise equipment, this method should be appropriate in calculating an estimate of the Young's modulus.

Beam and Loading	Elastic Curve	Maximum Deflection
		$-\frac{PL^3}{3EI}$
		$-\frac{wL^4}{8EI}$
		$-\frac{ML^2}{2EI}$
		$-\frac{PL^3}{48EI}$

**FIGURE 1: LIST OF BEAM LOADING CONFIGURATIONS WITH DEFLECTION EQUATIONS [2].**

## THEORY

### 1. Euler-Bernoulli beam theory

When analyzing a beam, the time and resources required to calculate its mechanics and simulate its behavior can be significantly simplified by making some assumptions and applying the Euler-Bernoulli beam theory [1]. Although there are more accurate techniques to analyze beam mechanics such as finite element analysis, they are significantly more complex and require additional computational power. The simplicity of the Euler-Bernoulli beam theory allows it to act as a quick and valuable insight tool.

In an ideal scenario, the beam would be of infinite length, have identical cross sections, and bend equally at every point of the long axis. This behavior is called pure bending, which does not account for shears, deformations, and bending effects [1].

The following are the assumptions that must be made in order to apply said beam theory:

1. The beam is infinitely rigid
2. Each beam cross section does not deform
3. The beam cross section is always perpendicular to the beam axis

With these assumptions, the Young's modulus can be calculated from the following equation [3]:

$$w = \frac{PL^3}{48EI} \quad (1)$$

where moment of Inertia ( $I$ ), Force applied ( $P$ ), length of the beam ( $L$ ) and the deflection ( $w$ ) are known. Rectangular beams were used in this lab, with the following moment of Inertia [4]:

$$I = \frac{bh^3}{12} \quad (2)$$

By inserting Eqn. (2) into Eqn. (1) and manipulating the result, we can get the following:

$$E = \frac{PL^3}{4wbh^3} \quad (3)$$

### 2. Uncertainties

The accuracy of the Euler-Bernoulli beam theory is limited not only by the assumptions stated, but also by the data used when applying the actual theory. Therefore, it is important to know the quality of the measurements taken to completely describe the theory's results and its accuracy. Statistical analysis of

error shows that there are multiple ways of estimating a measurement's errors based on using different probability distributions, the number of samples taken on a measurement, and the level of confidence, among other things [2].

One such model to estimate the precision uncertainty of a value (say  $x$ ) is:

$$P_x = t_{\frac{\alpha}{2},v} \frac{S_x}{\sqrt{n}} \quad (4)$$

at a confidence level of  $c\%$ .

One way to estimate the uncertainty of an instrument is to compare its measurements to a "standard," trustworthy instrument and take the root mean square (RMS) of the differences between the two measurements.

Further statistical analysis of uncertainty states that because of the fact that several, individual measurements with their own uncertainties are combined together to form a new calculated measurement, there exists a propagation of uncertainty given by the form:

$$u_x = \sqrt{\sum_{m=1}^n \left( \frac{\delta X}{\delta v_m} u_m \right)^2} \quad (5)$$

## PROCEDURES

### 1. Equipment

- ☐ Calipers
- ☐ FC22 Compression Load Cell
- ☐ EM1 Transmissive Optical Encoder
- ☐ Shop Vise with a Beam Support Attachment
- ☐ Weights
  - ☐ 25.02 lb
  - ☐ 50 lb
- ☐ Load Cell Calibration Rig
- ☐ NI BNC-2120 Connector Block
- ☐ NI PXI-6251 M Series Multifunction DAQ
- ☐ NI LabView

### 2. Calibration

In order to ensure accurate measurement and data collection, the testing equipment had to be properly set up and calibrated prior to the testing procedure. This consisted of calibrating an FC22 compression load cell and an EM1 trans-missive optical encoder module. In order to minimize human error during calibration, LabView was used in conjunction with human measurements.

To calibrate the FC22 load cell, a LabView VI was created to capture N samples of an A/D converter taken from an NI BNC-2120 connector block and output the average of each signal. The load cell was removed from the vise and was set up in a circuit such that +5V were applied to the cell while being connected to a NI PXI-6251 M Series DAQ. The load cell was then placed in a test rig consisting of a 0.4626 kg (1.02 lb) arm, resting on the load cell, where additional (known) weights can be placed. Using a LabView VI, multiple data sets of each tested weight combination were collected and compared against the measured voltage of the load cell. Applying a MATLAB polyfit on this data provides the offset and sensitivity of the load cell needed for the calibration.

After calibrating the encoder, the linear optical encoder readings and caliper measurements were compared to validate the calibration data. Running another LabView VI Lab 2 Sp2017.vi to acquire displacement data, the crosshead was lowered to a large displacement relative to the predicted testing conditions. The position of the crosshead was then measured with calipers again. These distances measured by the calipers were compared against the VIs output distances.

### 3. Testing

Beam bending tests could begin after the load cell was calibrated and the linear optical encoder readings validated. Three samples of thicknesses 0.156, 0.314, and 0.482 cm were each placed on two rods 8.992 cm apart and tested seven to ten times in the following manner:

1. The previously tested encoder is attached to a vise with a beam supporting attachment consisting of two rods
2. The sample is placed on the two rods, with the load cell directly above the center of the sample
3. The load cell is lowered such that it is slightly above the sample
4. The LabView VI "Lab 2 Sp2017.vi" is run with a sample size of 100,000, and a load cell offset [V] and sensitivity [V/lb] as calculated during calibration
5. While the VI is running, the load crosshead is lowered to bend the beam slightly

#### CAUTION:

The amount of deflection of the beam and the load on the beam should be noted. If the deflections are too large the assumptions of Euler-Bernoulli beam theory fail to hold due to plastic deformation (Young's modulus does not apply to plastic deformation cases). Overloading the load cell can result in inaccurate results and/or damage the load cell

6. After the VI comes to a stop, unload the sample
7. Repeat steps 3 to 6 until a satisfactory number of tests are run for each sample

## RESULTS AND DISCUSSION

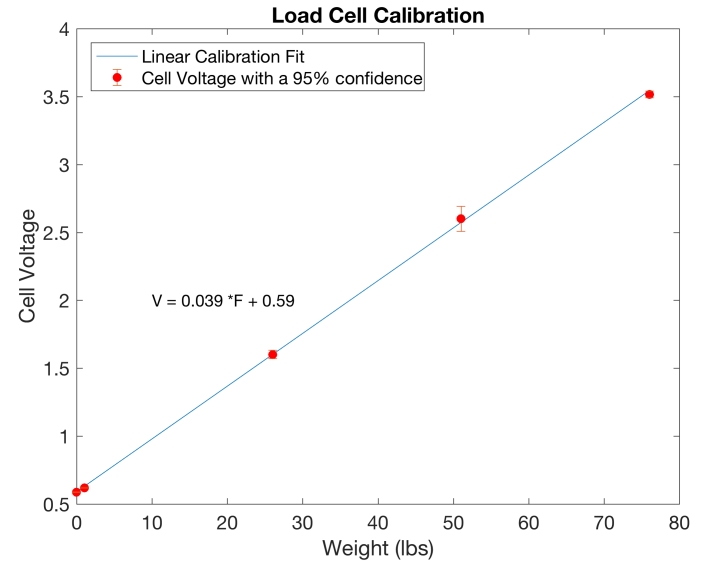


**FIGURE 2: LOAD CELL CALIBRATION BEST FIT GRAPH: RED LINES INDICATE 95% CONFIDENCE RANGE OF CELL VOLTAGE**

A line of best fit of the load cell calibration data, shown in Fig. 2, was taken to find the offset and sensitivity. In MATLAB, a *polyfit* of the data was taken. Note that the y-intercept is the DC offset, and the slope is the sensitivity. The results are shown in Table 1.

**TABLE 1: LOAD CELL CALIBRATION RESULTS**

DC offset [V]	0.5906
Sensitivity [V/lb]	0.0389

The full collection of data is summarized in Fig. 4, Fig. 5, and Fig. 6 in Appendix A. The voltage in the x-axis is linearly proportional to the magnitude of displacement.

The staircase appearance of Fig. 6 is also present in Fig. 4 and Fig. 5, though to a much lesser degree. Figure 4 is notably the smoothest. This is due to the different ranges of voltages covered; the smaller the range, the more noticeable the resolution of the data. The time step between the plots is more apparent when zoomed into a smaller voltage range. Figure 6 has a voltage

axis range that is one third the size of Fig. 4. Thus, the staircase appearance is zoomed in three times more in Fig. 6 than Fig. 4. With this in mind, the three sample plots were further analyzed.

The Young's modulus for each sample, calculated using Eqn. (3), is shown in Table 4.

The average Young's Modulus calculated for each sample is notably different from each other. However, the Young's Modulus of the samples should be the same, at around 69 GPa [5]. Thus, the uncertainty propagation must be analyzed to see if our results are within a reasonable range from the actual value.

Once the load cell was calibrated, the three samples were tested. The LabView VI "Lab 2 Sp2017.vi" generated plots for these data sets that appear as expected. The displacement showed as negative because the displacement was in the downwards direction. The relationship between the force and displacement is linear, as shown in Fig. 3. The slope should be representative of the Young's modulus. However, as shown at the rightmost part of the force-distance plot in Fig. 2, there are various sections of the data that are not linear. These correlate with when the load cell is not yet in contact with the beam, and when the beam approaches its yield stress. Sudden irregularities caused by external disturbances were also omitted. These portions are not representative of the Young's modulus, and is thus is not used in any of the following calculations.

The uncertainties associated with caliper measurements (i.e.  $u_b$ ,  $u_L$ ) were found by taking a standard deviation of the measurements for the thickness and the length of the beam. However, the standard deviation was 0, so the standard uncertainty of the caliper was used instead:

$$u_{cal} = \frac{0.001}{\sqrt{3}} \quad (6)$$

The uncertainty of the thickness of the sample ( $u_h$ ) was found by taking the standard deviation and multiplying it by the confidence interval range. For a 95% confidence level, the coefficient is 4.303. If the standard deviation turned out to be 0, then the calipers standard uncertainty was used again.

To find the uncertainty of the optical encoder ( $u_w$ ), the measurements taken from the VI was compared against the measurements taken from the caliper. The reported value of  $u_w$  is the RMS difference between the two measurements. Lastly, the load cells uncertainty was found by applying various weights and relating them to the composite standard deviation and grand mean for each voltage associated with it.

As error is known to propagate with respect to its measurements, Eqn. (5) and Eqn. (3) are combined to yield:

$$\frac{u_E}{E} = \sqrt{\left(\frac{1}{p}u_p\right)^2 + \left(\frac{1}{w}u_w\right)^2 + \left(\frac{3}{L}u_L\right)^2 + \left(\frac{1}{b}u_b\right)^2 + \left(\frac{3}{h}u_h\right)^2} \quad (7)$$

The calculated Young's modulus along with its uncertainty propagation are listed in Table 3.

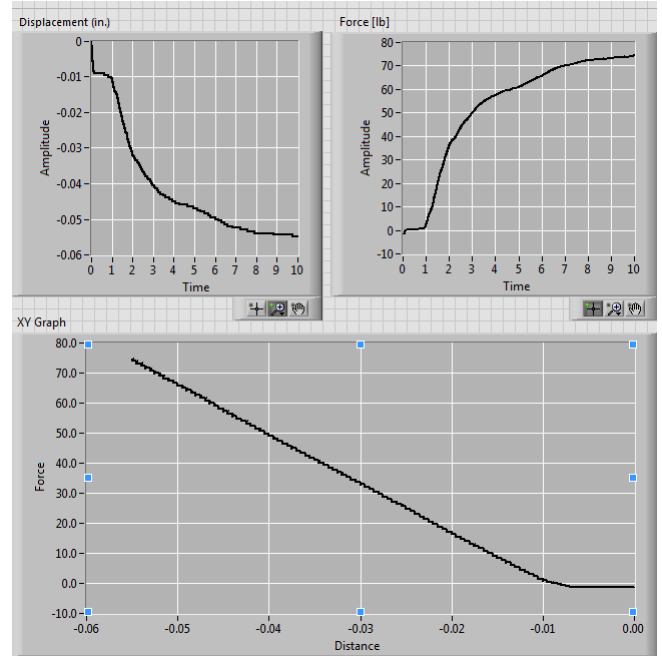


**FIGURE 3: LOAD FORCE AND DISPLACEMENT PLOTS FOR MEDIUM THICKNESS SAMPLE**

**TABLE 2: RELATIVE UNCERTAINTIES**

$u_h$ [cm] (thin)	0.0029
$u_h$ [cm] (medium)	0.00058
$u_h$ [cm] (thick)	0.00058
$u_b$ [cm]	0.00058
$u_L$ [cm]	0.00058
$u_w$ [cm]	0.0024
$u_p$ [N]	11

**TABLE 3: YOUNG’S MODULUS 95% RANGE**

Sample	95% C.I. (GPa)
Thin	$61.15 \pm 0.60$
Medium	$66.30 \pm 0.51$
Thick	$54.12 \pm 0.51$

## CONCLUSION

The calculated Young’s modulus isn’t within the reasonable range of values after calculating the uncertainty. This indicates that the testing method was not effective.

To improve the experimental procedure, individual uncertainties of the measurements need to be reduced to minimize the propagation of uncertainties in our final result. Ideally, the calibration of the encoder can be done with a larger sample size of data by having a wider variety of weights. In the lab setup, there were 3 weight sizes (10, 25 and 50 lbs) but with a more extensive experiment there should be more weight sizes and an even more accurately calibrated encoder. More precise measuring tools would also reduce the individual uncertainties.

During the loading of the material, a steady increase in the load as well as a limit upon the load on the material would prevent measurement error and overloading the samples. Further, the load cell is unable to process loads over 45.3592 kg (100 lbs), so using a load cell with a greater sensitivity range could prevent overloading errors.

With these results, another test on aluminum with a lower uncertainty and less potential disturbances would provide valuable data on the test’s ability to obtain the Young’s modulus. More testing samples in a well monitored environment would better represent the testing methods. The test procedure can also be applied to a variety of other materials other than aluminum, as long as the material is rigid enough to hold up to the initial assumptions.

## REFERENCES

- [1] Bauchau O.A., and Craig J.I., 2009 *Structural Analysis with Applications to Aerospace Structures*, Springer Netherlands, Dordrecht
- [2] Beckwith T.G., Marangoni R.D., and Lienhard J.H., 1993 *Mechanical Measurements*, 5<sup>th</sup> ed., Addison-Wesley Publishing Company, Inc., Boston
- [3] Beer F., and Johnston E.R., 2010. *Statics and Mechanics of Materials*, 1<sup>st</sup> ed., McGraw-Hill Education, NY
- [4] Coddington R., 2014. "Moment of Inertia". On the WWW, Feb. URL <http://abe-research.illinois.edu>.
- [5] MakeItFrom, 2016. "6061-T6 Aluminum". On the WWW, Feb. URL <http://www.makeitfrom.com>.

## Appendix A: Data results

**TABLE 4: CALCULATED YOUNG’S MODULUS (GPa)**

Test #	Thin	Medium	Thick
1	62.20	66.79	54.92
2	62.39	66.94	54.47
3	61.70	66.83	53.55
4	62.72	66.70	52.95
5	61.90	65.66	54.30
6	60.75	65.97	54.07
7	60.27	65.81	54.60
8	60.67	65.71	N/A
9	61.24	65.75	N/A
10	61.06	65.67	N/A
<b>Average</b>	<b>61.15</b>	<b>66.30</b>	<b>54.12</b>

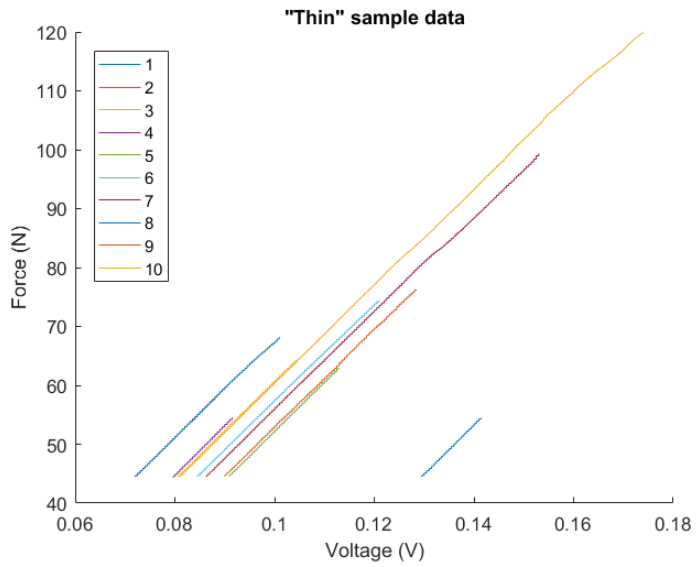


**FIGURE 4:** THIN SAMPLE GRAPH OF FORCE VS VOLTAGE

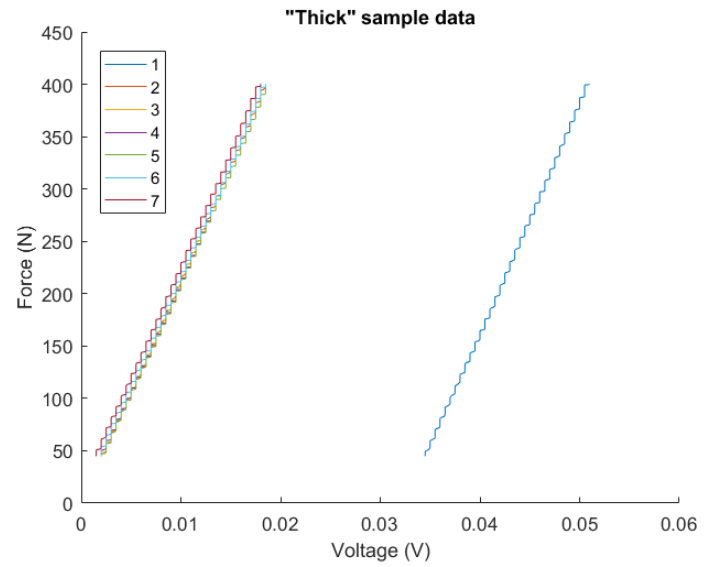


**FIGURE 6:** THICK SAMPLE GRAPH OF FORCE VS VOLTAGE

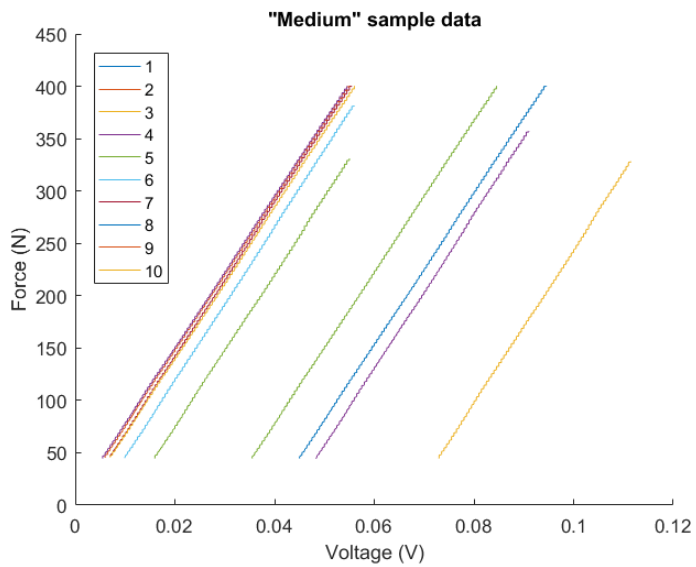


**FIGURE 5:** MEDIUM SAMPLE GRAPH OF FORCE VS VOLTAGE